IOP Conf. Series: Materials Science and Engineering **121** (2016) 012018 doi:10.1088/1757-899X/121/1/012018

Comparison of Two-Phase Pipe Flow in OpenFOAM with a Mechanistic Model

Adrian M Shuard[1], Hisham B Mahmud[2], Andrew J King[3]

[1] Mechanical Engineering Department, [2] Petroleum Engineering Department, Curtin University Sarawak, Miri, Malaysia

[3] Mechanical Engineering Department, Curtin University, Perth, Australia

E-mail: adrian.mark@postgrad.curtin.edu.my

Abstract. Two-phase pipe flow is a common occurrence in many industrial applications such as power generation and oil and gas transportation. Accurate prediction of liquid holdup and pressure drop is of vast importance to ensure effective design and operation of fluid transport systems. In this paper, a Computational Fluid Dynamics (CFD) study of a two-phase flow of air and water is performed using OpenFOAM. The two-phase solver, interFoam is used to identify flow patterns and generate values of liquid holdup and pressure drop, which are compared to results obtained from a two-phase mechanistic model developed by Petalas and Aziz (2002). A total of 60 simulations have been performed at three separate pipe inclinations of 0°, $+10^\circ$ and -10° respectively. A three dimensional, 0.052m diameter pipe of 4m length is used with the Shear Stress Transport (SST) $k-\omega$ turbulence model to solve the turbulent mixtures of air and water. Results show that the flow pattern behaviour and numerical values of liquid holdup and pressure drop compare reasonably well to the mechanistic model.

1. Introduction

Two-phase flow is a particular class of multiphase flow that is limited to the relative motion of two phases of immiscible fluids with different physical properties. It is common in many industrial applications such as power generation, oil and gas transportation and combustion systems. The prediction of liquid holdup and pressure drop in two-phase pipe flow is of vast importance during the design and operation stages in all applications to ensure the fluid system does not deviate from its operational envelope and cause damage to personnel, plant and equipment. Currently, steady-state hydrodynamic modelling is a technique that is widely used to help explain the behaviour and characteristics of two-phase flow [1].

Current methods for hydrodynamic modelling of two-phase flow typically comprise of either empirical or mechanistic models. Empirical models such as the well-known Beggs and Brill method [2] are an improvement of earlier homogeneous models as they provide a basis for the creation of flow regime maps and contain specific correlations for calculating liquid holdup and pressure drop. Empirical models are however based exclusively upon experimental data and are generally limited by the range of data on which they are based [3]. Alternatively, a mechanistic model is based on fundamental laws and observations and can typically offer more accurate modelling. A mechanistic transport equation is generally written for each of the phases in the system and best estimate mechanistic or correlational sub-models are used for parameters which

are substituted into the equations [4]. This makes the underlying mathematics of the mechanistic model readily accessible for future amendments.

Taitel and Dukler [5] produced the first widely used two-phase mechanistic model as an analytical prediction of the transition between flow regimes in circular pipes at different inclinations. The results from the model were validated with experimental observations conducted by Mandhane et al. [6]. Many efforts have since been focused on increasing the accuracy of the analytical prediction of the flow patterns and transition boundaries such as the work of [7], [8] and [9]. The latest significant edition is the Petalas and Aziz comprehensive mechanistic model [10], which has been upgraded to apply to all pipe geometries and fluid properties. Included in the model are various amendments to parameters such as the interfacial friction factor and the effects of wall roughness and liquid entrainment have been added. The model has compared well to data from the Stanford Multiphase Flow Database [11], which consists of over 1800 experiments using actual well data and over 20,000 laboratory measurements. The high level of validation makes the Petalas and Aziz mechanistic model ideal for comparison to Computational Fluid Dynamics (CFD) models. If a good comparison is shown the models can then be used to gain a more comprehensive understanding of the flow.

The use of CFD to numerically solve flow problems has proliferated in recent years due to the advent of increased computing power and more accessible parallel computing options. Numerous examples exist of CFD analysis of two-phase flow in straight pipes however studies are usually limited to 2-dimensional analysis such as [12], or are limited in scope to a single flow regime ([13], [14]). Examples for 3-dimensional analysis of multiple flow regimes typically use different numerical models depending on the specific flow regime under investigation such as [15]. This is due to the complexity for a single solver to accurately model the behaviour of changing flow regimes. Bestion [16] summarized the challenges when attempting to use a system wide 2-phase CFD solver for multiple flow regimes when considering thermal-hydraulics of nuclear reactors. It was reported that the system wide code was typically limited to producing a macroscopic description of the flow, whereby calibration of the code is usually required if small scale effects need to be resolved accurately. In addition, the majority of CFD studies of two-phase flow have typically been attempted using the standard solvers in commercial software such as ANSYS CFX and ANSYS Fluent. In recent years OpenFOAM has gained traction as an alternative simulation tool to the common commercial software used due to the absence of licensing costs, automatic parallelisation capability and wide range of solvers available.

OpenFOAM is an open source C++ library consisting of solvers and utilities with the primary purpose for use in CFD applications. Two-phase flow is handled in OpenFOAM using interFoam, a transient solver for two incompressible, isothermal and immiscible fluids using an interface capturing technique based a modified Volume of Fluid (VOF) approach first introduced by Hirt and Nichols [17]. Validation of the interFoam solver has so far been confined to the specific interest of users and its applicability to a wide range of multiphase flow applications is yet to be established. Deshpande et al. [18] presented a summary of completed interFoam validation efforts and added further validation for pure advection, high Weber number flows and surface tension dominated flows. Any further review of the literature suggests that the use of interFoam to model two-phase pipe flow is scarce and has also been confined only to visual inspection of flow patterns based upon a specified flow map. Herreras and Labeaga [19] simulated two-phase flows of air and water in open and closed channels at different inclinations with comparison to the Taitel and Dukler flow map. Reported results however, were inaccurate due to a low mesh density and lack of a three-dimensional model. Thaker and Banerjee [20] performed a three-dimensional numerical simulation of air and water flow in a 10mm diameter, 1.5m long horizontal pipe where flow pattern results were compared by visual inspection to the experimental work of Vaze and Banerjee [21]. Results for the stratified, slug, plug and annual flow patterns compared well visually to the experimental results however no attempt was made to obtain and compare

values of liquid holdup and pressure drop.

In this paper it is proposed to further compare and validate the CFD simulation results obtained using the interFoam solver by comparing values of pressure drop and liquid holdup for two-phase flow at 0°, +10° and −10° inclinations to the Petalas and Aziz mechanistic model. Simulation points are selected such that comparisons can be made for the stratified wavy, slug, dispersed bubble, froth and annular flow regimes. The purpose is not to provide the most accurate analysis of each flow pattern but rather to determine whether a system wide CFD solver such as interFoam can be used with a reasonable degree of accuracy across multiple flow regimes. Successful implementation of this will enable confidence that the CFD model presented here can be utilized for further studies such as optimisation of pipeline flow or may form the basis for further studies with different fluids and pipe geometries.

2. Numerical Approach

OpenFOAM 2.1.x was used to simulate the flow using the interFoam solver. The Steady State Transport (SST) $k-\omega$ turbulence model was selected for all simulations. A three-dimensional half-pipe model was constructed with a diameter of 0.052m and a length of 4m. The geometry and mesh were both constructed in SALOME 7.4.0 and exported to OpenFOAM via the ideasUnvToFoam utility. The mesh comprised of 352628 hexahedral elements and was selected such that the boundary layer was resolved in all simulations using 8 graded layers. Values of y+ for all simulations were obtained for both phases using the yPlusRAS utility and residuals were plotted using gnuplot, after extracting the final residual data located in the log file. Gravitational acceleration was applied in the vertical (Z) direction. Analysis was conducted on different pipe inclinations by altering the appropriate vector components of the gravitational acceleration in the g file contained in the constant file directory. Fig. 1 shows the topology of the mesh.

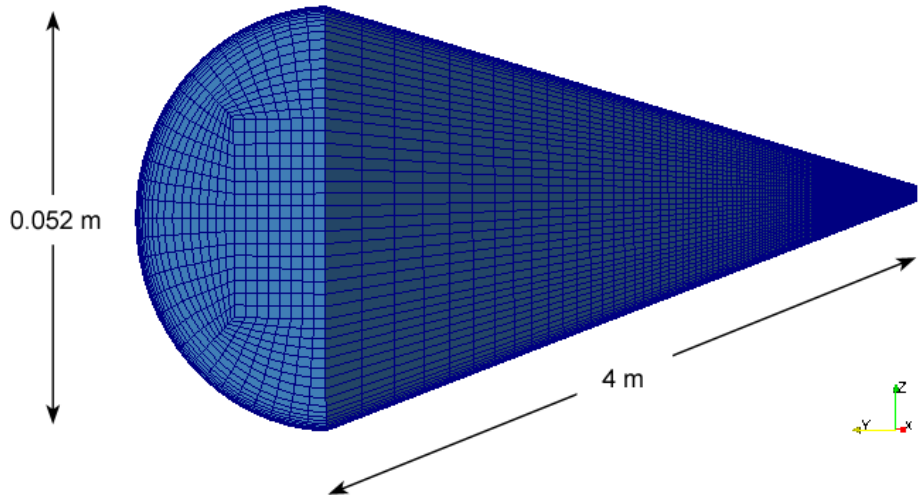

Figure 1. Mesh topology with coordinate system.

To ensure correct solution control an adjustable time step was used with an initial value of 1e-07s in conjunction with a MaxCo (mean Courant number) limit of 0.3 and a MaxAlphaCo (interface Courant number) limit set to 0.1. Standard numerical schemes for interFoam are used with the exception of *limitedLinearV 1* for the velocity component advection term to improve the solution stability. Calculations for pressure-velocity coupling are performed using the PIMPLE (merged PISO-SIMPLE) algorithm with five corrector loops and interface compression is used

for the determination of phase fraction to yield a sharp interface. Other main system parameters used in the analysis are shown in Table 1.

Table 1. System parameters.

Parameter	Value
Air density	1 $[kg/m^3]$
Water density	1000 $[kg/m^3]$
Air kinematic viscosity	1.48e-05 $[m^2/s]$
Water kinematic viscosity	1e-06 $[m^2/s]$
Interfacial tension	7.24e-02 $[N/m]$
Pipe roughness (absolute)	4.57e-04 $[m]$

All results obtained from this analysis were viewed and analysed using ParaView, an open-source, multi-platform data analysis and visualisation application.

2.1. Boundary conditions
In all simulations the velocity was specified as *fixedValue* at the inlet and *zeroGradient* at the outlet. Conversely, the pressure was specified as *zeroGradient* at the inlet and *fixedValue* at the outlet. A no-slip boundary condition is applied to the pipe wall by setting the velocity as zero and a symmetry boundary condition was imposed at the longitudinal section of the half-pipe in the X-Z plane shown previously in Fig. 1. A summary of the boundary conditions used for all simulations are listed in Table 2.

Table 2. Boundary conditions.

Parameter	Inlet	Outlet	Wall
U	fixedValue	zeroGradient	fixedValue uniform 0
p_rgh	zeroGradient	fixedValue uniform 0	zeroGradient
k	fixedValue	zeroGradient	fixedValue
nut	Calculated uniform 0	Calculated uniform 0	nutkRoughWallFunction
omega	fixedValue	zeroGradient	omegaWallFunction

The pipe was initially filled with water and an equal fraction of air and water was introduced at the inlet upon commencement of the simulation (t=0s). Simulations were run until both phases had time to pass from the inlet through the entire length of the pipe. Values of liquid holdup and pressure drop were obtained from a point defined by the turbulent entrance length of each phase based on the inlet superficial velocity (whichever was greater) to a point 0.5m from the pipe outlet to reduce any inlet and outlet pressure effects.

2.2. Symmetry and mesh independency analysis
Prior to commencement of the comparative study, three simulations were run on a full 3D horizontal pipe for stratified wavy, slug and dispersed bubble flow to determine the suitability of using a symmetric boundary condition. Fig. 2a shows the longitudinal (U_x) and lateral (U_y) velocities per radial distance (sampled in the Z direction) for stratified wavy flow at the midpoint of the pipe (inlet velocities: $U_{sg} = 2$ m/s, $U_{sl} = 0.5$ m/s). The results clearly show that negligible mass flow exists across the geometric mid-plane while the behaviour of the longitudinal velocity

is consistent for two-phase stratified wavy flow with a faster gas phase [20]. It has been concluded that the symmetric boundary condition applied in this study is applicable as the velocity vector across the mid-plane was also observed to be zero for all other flow patterns considered.

A mesh independency analysis was performed by comparing values of liquid holdup and pressure drop with the mesh cell count for the stratified, slug and elongated bubble flow patterns. The cell count was increased until the obtained results were less than 5% of the previous case and good agreement with the mechanistic model was achieved. Fig. 2b shows the evolution of the pressure drop depending on the total mesh cell count for a stratified wavy flow (inlet velocities: $U_{sg} = 2$ m/s, $U_{sl} = 0.5$ m/s).

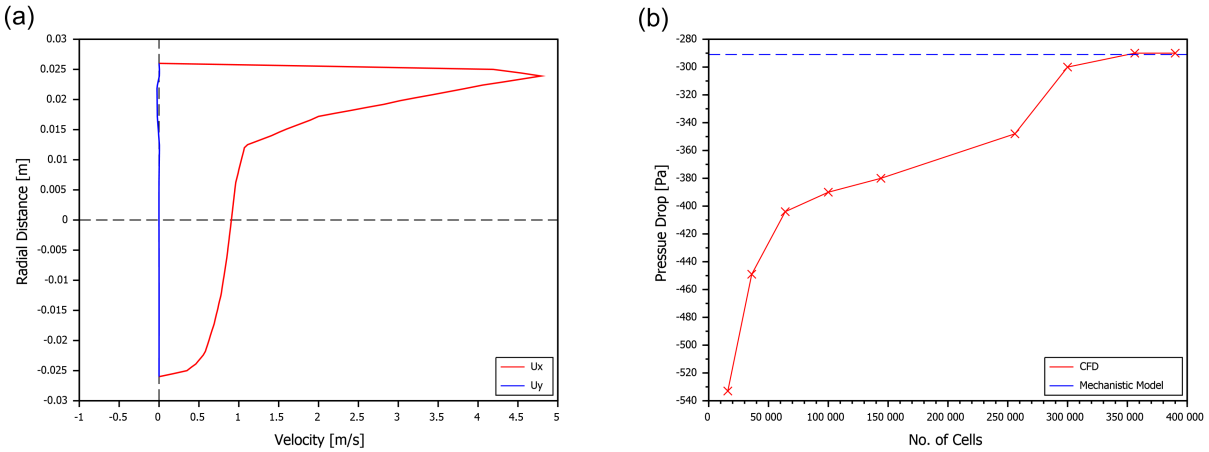

Figure 2. (a) Longitudinal and lateral velocity at the pipe midpoint for stratified wavy flow (inlet velocities: $U_{sg} = 2$ m/s, $U_{sl} = 0.5$ m/s), (b) Evolution of the pressure drop depending on the total mesh cell count for stratified wavy flow (inlet velocities: $U_{sg} = 2$ m/s, $U_{sl} = 0.5$ m/s) with a comparison to the theoretical pressure drop obtained from the mechanistic model.

2.3. Simulation points

20 simulations have been performed for each separate pipe inclination bringing the total to 60 simulations conducted. The different superficial inlet velocities for the liquid and gas phases are shown superimposed on the approximate flow regime map in Fig. 3, whereby a) is for the horizontal pipe, b) the $+10°$ inclined pipe and c) the $-10°$ declined pipe respectively. The flow regime map for each inclination has been determined by the Petalas and Aziz mechanistic model.

3. Results

3.1. Flow pattern visualisation

The general types of visualisation generated in the analysis; stratified wavy, slug, dispersed bubble, froth and annular mist flow are presented graphically in terms of volume fraction of the water phase (alpha) in Fig. 4. The blue colour represents water (alpha = 1) and the black colour represents air (alpha = 0). The interface between the two phases is represented by the white colour (alpha = 0.5).

Stratified Wavy: Results show a good visual correlation in all cases between the CFD results and the flow pattern identified by the mechanistic model. Waves form periodically at the interface and are carried downstream. An increase in the liquid inlet velocity correctly yielded

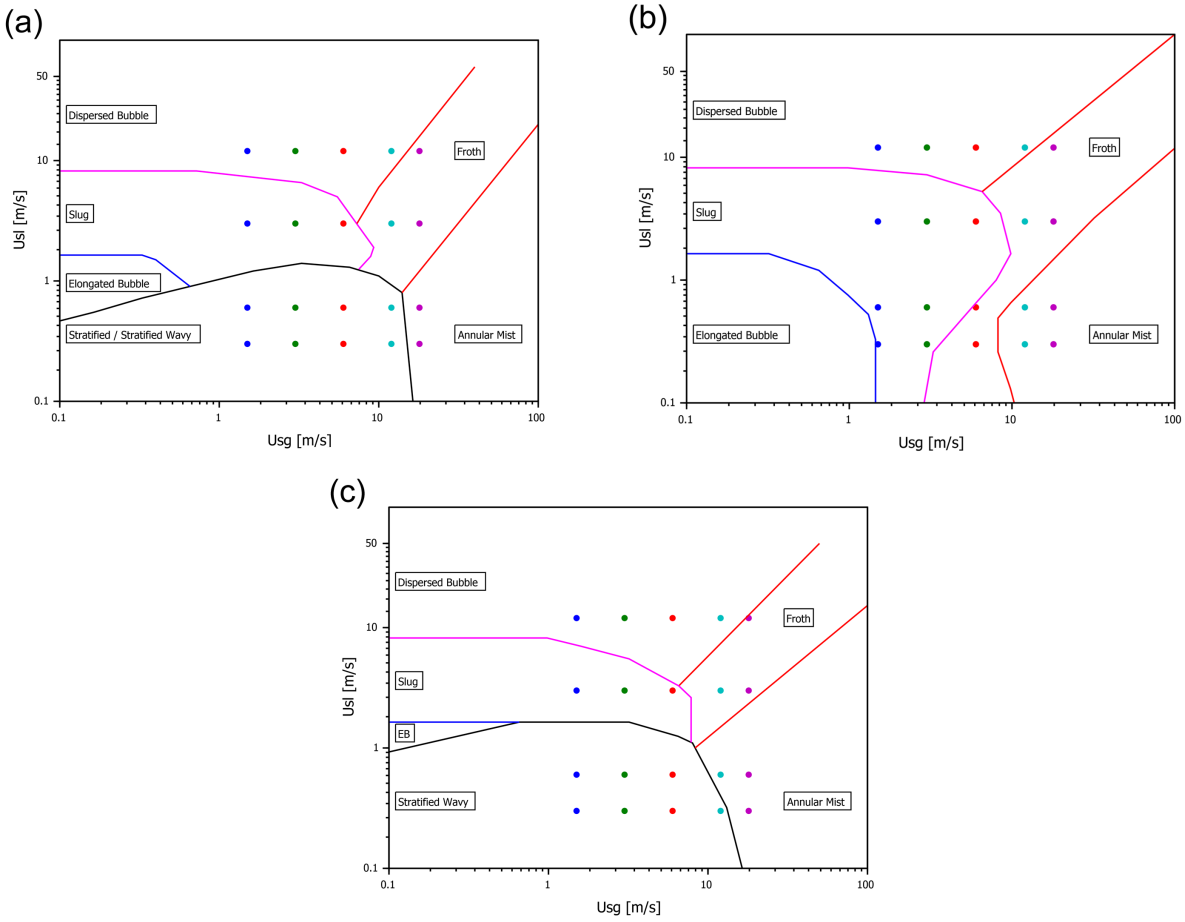

Figure 3. Petalas and Aziz flow regime maps with superimposed CFD simulation points for; (a) horizontal flow, (b) $+10^{\circ}$ (inclined) flow, (c) -10° (declined) flow.

an increase in liquid holdup while an increase in the gas velocity yielded a decrease in liquid holdup. Wave height was shown to be dependent on the velocity difference of the two phases as postulated in the Kelvin-Helmholtz wave instability theory [22]. The -10° declined pipe correctly predicted a reduction in the liquid holdup for all cases and stratified flow was correctly shown not to exist in the $+10^{\circ}$ inclined pipe.

Slug: The existence of slug flow was predicted correctly for all simulations with visualisation results closely matching numerical and experimental studies reported in the literature [23]. Slug flow was initialised by a wave forming at the interface. As the liquid velocity was greater than the stratified flow cases the liquid holdup was increased and waves that were formed were high enough to impact on the top pipe surface causing periodic slugging to occur at regular intervals. The effect of gravity was evident with slugging occurring at lower liquid velocities in the $+10^{\circ}$ inclined pipe.

Dispersed Bubble: In the dispersed bubble flow regime, the liquid height quickly reaches the top surface of the pipe whereby small groups of air bubbles were observed to be entrained in the main fluid body and carried downstream. The longitudinal mesh density was not fine

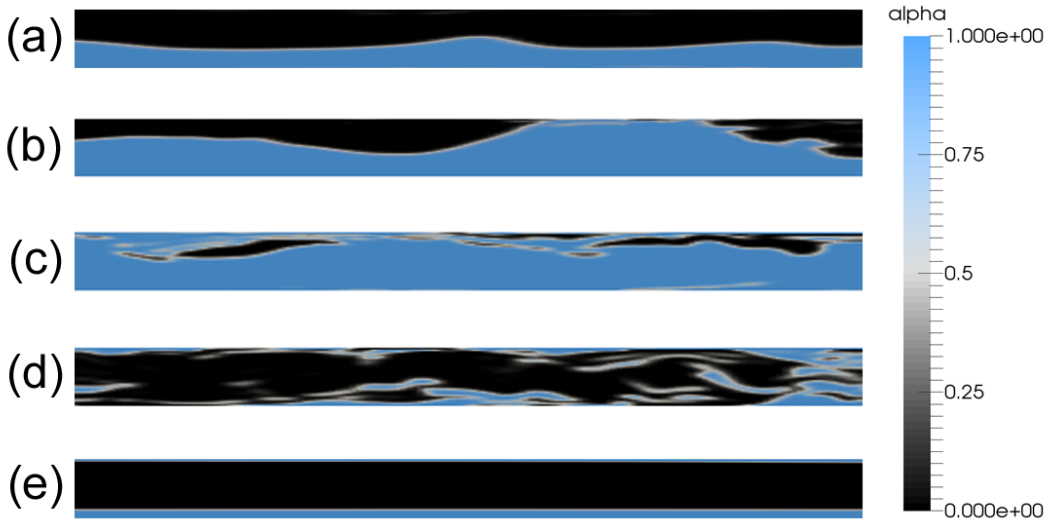

Figure 4. Flow pattern visualisation for (a) stratified wavy, (b) slug, (c) dispersed bubble, (d) froth and (e) annular mist flow.

enough to capture all the detailing on the bubbles which appear to coalesce and elongate in this study as opposed to being purely spherical as defined in the literature [24]. Pipe inclination had a negligible effect on the visualisation.

Froth: The visualisation of froth flow deviated significantly from results reported in experimental studies [25]. Froth flow comprised of wispy areas of elongated water contained within the air phase. The visual results however, were significantly different from all other flow pattern visualisations and thus can be said to match the mechanistic model predictions. Froth flow was initiated by an increased gas phase velocity which caused an initial liquid wave to quickly reach the top surface of the pipe where it was broken up and carried downstream in elongated liquid streaks.

Annular Mist: All existences of the annular flow patterns were consistent with the mechanistic model prediction. The visualisation correctly consisted of a layer of fluid at the radial extremity of the pipe with an annular core of high velocity gas; however no evidence of mist existed in the core due to the limited mesh size. The lower section of the layer was observed to be noticeably thicker due to the influence of gravity which is consistent with other experimental studies completed [26].

3.2. Liquid holdup and pressure drop comparison

Values of liquid holdup and pressure drop depending on flow regime are presented for both the CFD and mechanistic model in Figs. 5 and 6 where; a) stratified wavy, b) slug c) elongated bubble, d) froth, e) annular mist and f) represents the results from the complete set of 60 simulations with $\pm 10\%$ error margins included. The vertical lines on the plots indicate the difference between the values form the CFD analysis and mechanistic model. In this representation, the specific velocity input value for each specific phase can be deduced from the Fig. 3 flow maps whereby the simulation number from Figs. 5 and 6 represents the simulation point from Fig. 3 when read from left to right, starting from the lower left most point in the flow pattern zone. Dotted lines are used in Figs. 5 and 6 to indicate consecutive simulations that are at the same inlet liquid superficial velocity as referenced by the flow maps.

3.3. Average error magnitude
Values of the average error magnitude for liquid holdup and pressure drop depending on pipe inclination and flow pattern type are presented in Fig. 7.

4. Discussion
It is shown that the effect of changing pipe inclination is to shift the flow regime boundaries on the flow pattern map. The boundaries of flow patterns such as stratified wavy, elongated bubble, slug and froth flow are particularly influenced by changes in inclination whereas dispersed bubble and annular mist exhibit little change. The OpenFOAM simulations correctly depicted the changes in flow regimes when compared to the mechanistic model.

Stratified wavy flow was simulated for 8 cases using the horizontal pipe and 7 cases using the -10 declined pipe. A very good correlation is observed in all cases between the CFD and mechanistic model for the liquid holdup with a mean error of less than 8%, with error margins very similar for both horizontal and declined flow. A comparison of pressure drop showed good accuracy for all cases with the exception of points near the transition to annular mist flow. The effect of increasing the inlet gas velocity correctly translates to a reduction of liquid holdup and an increase in pressure drop.

Slug flow was simulated for a total of 12 cases across all three inclinations. Excellent accuracy of the liquid holdup is observed with an average error less than 6% compared to the mechanistic model with error margins similar across all inclinations. High pressure drop errors of 30% are observed in the horizontal and declined pipes whereby the increased accuracy evident in the inclined pipe is attributed to the three additional simulation points at a much lower liquid velocity which showed good correlation to the mechanistic model.

Dispersed bubble flow showed the most accurate results for the liquid holdup and pressure drop with a mean error less than 5% and 20% respectively. It is possible that this is due to the high liquid phase fraction of the flow aiding more accurate determination of the pressure drop due to a more viscous and dense combined flow. In addition, throughout all changes of pipe inclination the dispersed bubble regime is the least affected in terms of pressure drop variations. It can be seen that the flow pattern map remains roughly the same size as shown in Fig. 3. As this phase exhibits the least change it is the least affected by gravitational effects which could explain the lowest mean error.

Froth flow was simulated for 3 cases in the horizontal pipe, 5 cases for the inclined pipe and 3 cases in the declined pipe. Liquid holdup and pressure drop comparisons were generally good with less than 11% and 35% mean error respectively. Errors may be attributed to deviation in the flow pattern visualisation whereby the mesh density was not fine enough in the longitudinal direction to provide an accurate depiction of the flow.

Annular mist flow was simulated for a total of 9 cases. Results of the liquid holdup show the greatest error margin (<17%) compared to all other flow patterns considered. Mean errors in pressure drop were within 20-40% depending on the pipe inclination when compared to the mechanistic model. A good consistency is evident for liquid holdup across all inclinations with a variation of less than 1%. The highest pressure drop errors occurred in the inclined pipe and are attributed to the two additional simulation points near the flow boundary with the froth flow regime.

It can be seen that liquid holdup results are better for flows involving equal or higher flow rates for the liquid phase compared to the gas phase, with dispersed bubble flow showing the highest accuracy and annular mist flow being the least accurate. Regardless of flow regime, a good consistency in error margin is achieved between each inclination. This consistency is not immediately apparent when comparing errors in pressure drop, where large fluctuations are observed between each flow regime and inclination especially for simulation points located near flow regime boundaries. Despite this, overall it is seen that dispersed bubble flow exhibits the

least mean error as in the case of the liquid holdup.

This may be explained by the weighted average values for density and viscosity used by the interFoam solver when solving the Navier-Stokes equations. The high density and viscosity ratios of air and water could be a contributing factor in introducing erroneous disturbances in the air phase at high velocities. Despite the magnitude of the pressure drop error margins recorded, the overall results give confidence that interFoam, and its implementation of the modified VOF method using the SST $k-\omega$ turbulence model can be used to give reasonable solutions to two-phase flow across multiple flow regimes, especially stratified wavy, slug and dispersed bubble.

5. Future work

It is intended to apply the same methodology presented here to a two-phase flow of oil and gas. This will yield insight into how different density and viscosity ratios could affect the flow and allow OpenFOAM to be applied to more oil and gas specific applications.

6. Conclusion

60 separate CFD simulations for two-phase flow have been completed on an air/water mixture at three separate inclinations using the interFoam solver with comparison to the Petalas and Aziz mechanistic model. All flow patterns observed in the CFD analysis were consistent with the mechanistic model prediction; however dispersed bubble and froth flow deviated from observations reported in the literature due to the limited mesh density in the longitudinal direction. A good correlation exists for the values of liquid holdup, with the highest average error occurring in the annular-mist flow regime while dispersed bubble flow exhibited the best result correlation. Similarly, the average error in the pressure drop was also observed to be highest in the annular flow regime and least in the dispersed bubble flow regime. The following conclusions are made following the results of this study;

- interFoam as a system wide solver is capable of capturing changes in the various flow patterns with a reasonable degree of accuracy for liquid holdup and pressure drop.
- Changes in pipe inclination were accurately reflected in the CFD simulation.
- Greater accuracy for both liquid holdup and pressure drop is obtained in the presence of a high velocity liquid phase as opposed to a high velocity gas phase.
- Mesh density in the longitudinal direction must be finer to provide a more accurate visualisation of dispersed bubble and froth flow.
- Usage of the SST $k-\omega$ turbulence model with a resolved boundary layer is appropriate to describe the flow with the boundary conditions used.

Nomenclature

k	turbulence kinetic energy $[m^2/s^2]$
nut	turbulence viscosity $[m^2/s]$
omega	specific rate of dissipation $[1/s]$
p_rgh	static pressure minus dynamic pressure $[kg/m-s^2]$
U	velocity $[m/s]$
U_{sl}	superficial liquid velocity $[m/s]$
U_{sg}	superficial gas velocity $[m/s]$
U_x	velocity in the X (longitudional) direction $[m/s]$
U_y	velocity in the Y (vertical) direction $[m/s]$

References

[1] Shippen M and Bailey W J 2012 Steady-state multiphase flow - past, present, and future, with a perspective on flow assurance *Energy & Fuels* **26** pp 4145-57
[2] Beggs D H and Brill J P 1973 A study of two-phase flow in inclined pipes *J. Pet. Tech.* **25** pp 607-17
[3] Ellul I R, Saether G and Shippen M E 2004 The modeling of multiphase systems under steady-state and transient conditions - a tutorial *Proc. 36th PSIG Annual Meeting (Palm Springs)* PSIG-0403
[4] Finch F, Ellul I R and Gochnour R 1991 Implementation of mechanistic flow models in a practical multiphase flow simulator *Proc. 23rd PSIG Annual Meeting (Minneapolis)*
[5] Taitel Y and Dukler A E 1976 A model for predicting flow regime transitions in horizontal and near horizontal gas-liquid flow *AIChE Journal* **22** pp 47-55
[6] Mandhane J M, Gregory G A, and Aziz K 1974 A flow pattern map for gasliquid flow in horizontal pipes *Int. J. Multiphase Flow* **1** pp 537-53
[7] Barnea D, Shoham O, and Taitel Y 1982 Flow pattern transition for downward inclined two phase flow; horizontal to vertical *Chem. Eng. Sci.* **37** pp 735-40
[8] Xiao J J, Shoham O and Brill J P 1990 A comprehensive mechanistic model for two-phase flow in pipelines *Proc. SPE Ann. Tech. Conf. (New Orleans)* SPE-20631-MS
[9] Gomez L E, Shoham O, Schmidt Z, Chokshi R N, Brown A and Northug T 1999 A unified mechanistic model for steady-state two-phase flow in wellbores and pipelines *Proc. SPE Ann. Tech. Conf. (Houston)* SPE-20631-MS
[10] Petalas N and Aziz K 2000 A mechanistic model for multiphase flow in pipes *J. of Canadian Pet. Tech.* **39** pp 43-55
[11] Petalas N and Aziz K 1995 *Stanford multiphase flow database - user's manual* Stanford Uni.
[12] Desamala A B, Dasamahapatra A K, and Mandal T K 2014 Oil-water two-phase flow characteristics in horizontal pipeline - a comprehensive cfd study *Int. J. Chem., Molecular, Nuclear, Mat. and Metallurgical Eng.* **8** pp 360-364
[13] DeSampaio P A B, Faccini J L H, and Su J 2008 Modelling of stratified gas–liquid two-phase flow in horizontal circular pipes *Int. J. of Heat and Mass Trans.* **51** pp 2752-61
[14] Rzehak R and Kriebitzsch S 2015 Multiphase cfd-simulation of bubbly pipe flow: a code comparison *Int. J. of Multiphase Flow* **68** pp 135-52
[15] Vasquez F, Stanko M, Vasquez A, DeAndrate J, and Asuaje M 2012 *Advances in Fluid Mechanics IX* ed M Rahman and C A Brebbia (Southhampton: WIT Press) pp 381-92
[16] Bestion D 2014 The difficult challenge of a two-phase cfd modelling for all flow regimes *Nuclear Eng. and Des.* **279** pp 116-25
[17] Hirt C W and Nichols B D 1981 Volume of fluid (vof) method for the dynamics of free boundaries *J. Comp. Phy.* **39** pp 201-25
[18] Deshpande S S, Anumolu L, and Trujillo M F 2012 Evaluating the performance of the two-phase flow solver interfoam *Comp. Sci. & Dis.* **5** pp 1-36
[19] Labeaga J I and Omagogeascoa N H 2013 Two-phase pipeflow simulations with openfoam *MS thesis, Norwegian Uni. of Sci. Tech. (Trondheim)*
[20] Thaker J P and Banerjee J 2013 CFD simulation of two-phase flow phenomena in horizontal pipelines using openfoam *Proc. 40th Nat. Conf. on Fluid Mech. & Fluid Power (Hamipur)* FMFP2013 paper 34
[21] Vaze M J and Banerjee J 2011 Experimental visualization of two-phase flow patterns and transition from stratified to slug flow *J. Mech. Eng. Sci.* **225** pp 382-89
[22] Yih C S 1969 *Fluid Mechanics* (New York: McGraw-Hill) p 662
[23] Vallée C, Höhne T, Prasser H M, and Sühnel T 2008 Experimental investigation and cfd simulation of horizontal stratified two-phase flow phenomena *Nuc. Eng. and Des.* **238** pp 637-46
[24] Andreussi P, Paglianti A, and Silva F S 1999 Dispersed bubble flow in horizontal pipes *Chem. Eng. Sci.* **54** pp 1101-07
[25] Gajbhiye R N and Kam S I 2011 Characterization of foam flow in horizontal pipes by using two-flow-regime concept *Chem. Eng. Sci.* **66** pp 1536-49
[26] Kumar K, Thaker J P, and Banerjee J 2013 Experimental investigations on two-phase flow phenomena in horizontal pipe *Proc. 40th Nat. Conf. on Fluid Mech. & Fluid Power (Hamirpur)* FMFP2013 paper 34

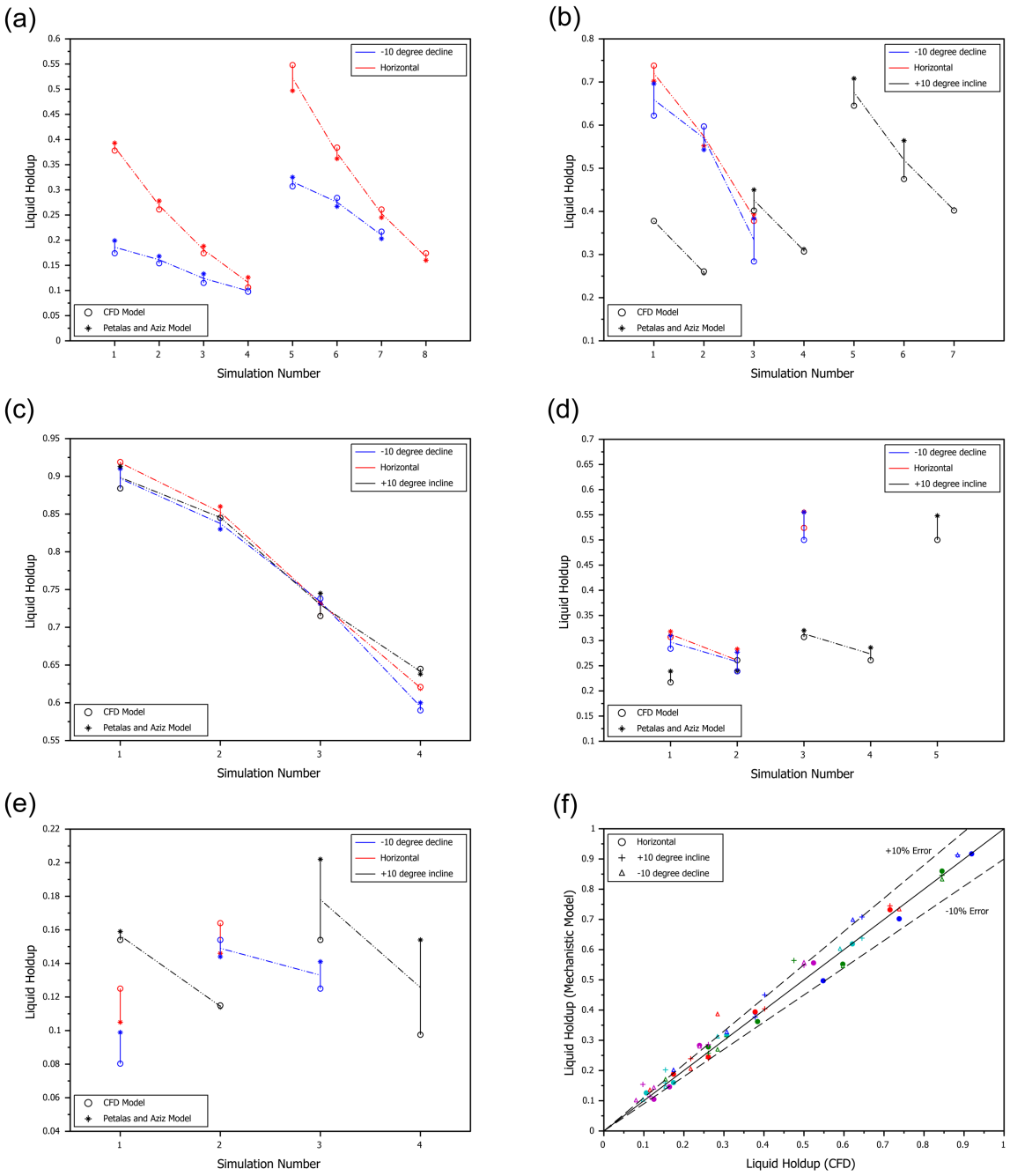

Figure 5. Liquid holdup results for each flow regime: (a) stratified wavy, (b) slug, (c) dispersed bubble, (d) froth and (e) annular mist; (f) represents a comparison of the complete data set for all inclinations with error margins shown.

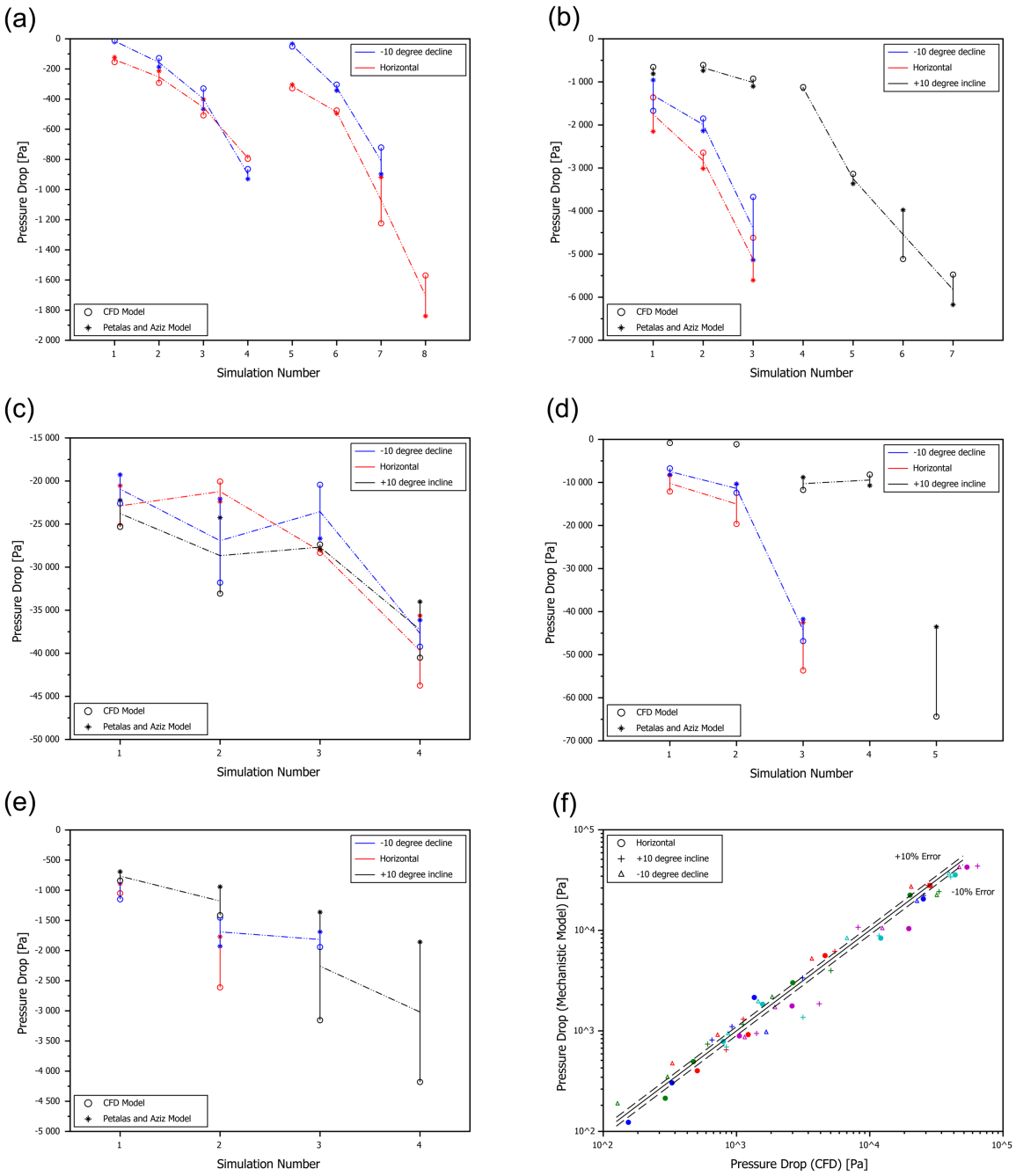

Figure 6. Pressure drop results for each flow regime: (a) stratified wavy, (b) slug, (c) dispersed bubble, (d) froth and (e) annular mist; (f) represents a comparison of the complete data set for all inclinations with error margins shown.

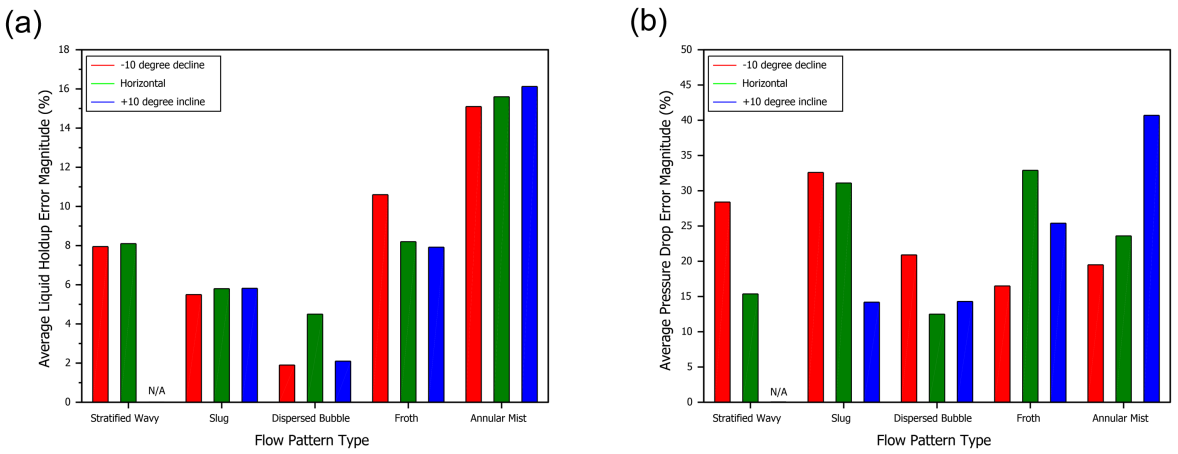

Figure 7. Average error magnitude for all flow regimes and inclinations; (a) liquid holdup and (b) pressure drop.